



ELSEVIER

Contents lists available at ScienceDirect

## Organic Electronics

journal homepage: [www.elsevier.com/locate/orgel](http://www.elsevier.com/locate/orgel)

# A new multicolored and near-infrared electrochromic material based on triphenylamine-containing poly(3,4-dithienylpyrrole)

Jian-Cheng Lai, Xin-Rong Lu, Bo-Tao Qu, Feng Liu, Cheng-Hui Li<sup>\*</sup>, Xiao-Zeng You<sup>\*</sup>

State Key Laboratory of Coordination Chemistry, School of Chemistry and Chemical Engineering, Nanjing National Laboratory of Microstructures Nanjing University, Nanjing 210093, People's Republic of China

## ARTICLE INFO

## Article history:

Received 18 September 2014

Received in revised form 20 October 2014

Accepted 21 October 2014

Available online xxxx

## Keywords:

Electrochromic

Near-IR

Poly(3,4-dithienylpyrrole)

Triphenylamine

Device

## ABSTRACT

A new compound containing both 3,4-dithienylpyrrole (DTP) and triphenylamine (TPA) groups, namely, 4'-(2,5-di(thiophen-2-yl)-1H-pyrrol-1-yl)-N,N-diphenylbiphenyl-4-amine (**DTP-Ph-TPA**), was designed and synthesized. The polymer poly-**DTP-Ph-TPA** (**PDTP-Ph-TPA**) was prepared by electropolymerization from **DTP-Ph-TPA**. When the applied potential circulates from 0.0 V to 1.4 V, the polymer not only exhibits reversible multicolor in the visible region (yellow, light green, magenta and blue), but also shows excellent electrochromic properties in the NIR region with high contrast ratio ( $\Delta T = 70.5\%$  in 1550 nm,  $\Delta T = 67.9\%$  in 1310 nm) and a very short response time (about 1.4 s for 1550 nm, 0.9 s for 1310 nm). A single layer electrochromic device (ECD) based on polymer **PDTP-Ph-TPA** was constructed and characterized.

© 2014 Published by Elsevier B.V.

## 1. Introduction

Electrochromic materials, which exhibit reversible absorption spectral changes by changing the applied potentials, have attracted much attention in recent years [1–8]. Originally, the research of electrochromic materials was mainly focused on the optical changes in the visible region (e.g., 350–750 nm), which had variable applications such as smart windows, E-paper, optical switching devices, variable reflectance mirrors, and camouflage materials. Later, efforts has also been made on near-infrared region (NIR; e.g., 750–2000 nm), which are useful in optical fiber-based telecommunication (specifically, 850 nm, 1310 nm and 1550 nm), optical attenuator, data storage, thermal control and aerospace and military camouflage [9–16]. Reynolds demonstrated color-to-transmissive NIR electrochromic conjugated polymers poly(3,4-propylenedioxythiophene)s

(PProDOTs) which showed essentially no color change in the visible region [9]. Wang and Wan reported a quinone-containing electrochromic materials, which showed high absorption in the NIR region in the range of 700–1100 nm by electrochemical reduction [10]. Liou made efforts on the triarylamine-containing electroactive aramids, which revealed highly stable electrochromism and high contrast ratio between NIR and visible light region [11–14]. However, so far there is less work on electrochromic materials that can function in both the UV–Vis and near-IR region [4], which makes it possible to monitor the near-IR electrochromic process through naked eye. Actually, it is a challenge to obtain a material that can be switched from highly transmissive state to highly absorbed state in a wide range from UV–Vis to near-IR region.

Typical electrochromic materials are coordination complexes, transition-metal oxides, organic molecules and conjugated polymers [4–6]. Among these different types of electrochromic materials, conjugated polymers have several advantages, such as multiple hues within the same material, absorption spectral tunability through structural

<sup>\*</sup> Corresponding authors.

E-mail addresses: [chli@nju.edu.cn](mailto:chli@nju.edu.cn) (C.-H. Li), [youxz@nju.edu.cn](mailto:youxz@nju.edu.cn) (X.-Z. You).

modification, flexibility, easy processability, fast switching, high optical contrast ratio and coloration efficiency [2]. Polythiophene, polypyrrole, polyaniline, poly(3,4-ethylenedioxythiophene) (PEDOT), poly(3,4-dithienylpyrrole) (PDTP), and their derivatives are the typical electrochromic conjugated polymers reported in literature [4,7]. Particularly, PDTP and its derivatives have become one of the most important electrochromic materials during the past 20 years [17–21]. They have many advantages over other conjugated polymers such as lower oxidation potentials (about 0.7 V vs SCE), sufficient electron density and good hole-transporting ability, and better film-forming properties. If the substituent group on the N-position were modified, they can show more electrochromic hues ranging from yellow [21,22], green [23], magenta [24], and cyan [25], to blue [23]. So far, most of the PDTP derivatives can show electrochromism only in the UV–Vis region, electrochromic PDTP polymers which can exhibit reversible absorption changes in both the near-IR region and UV–Vis region are scarce [4].

In the literature, two groups were typically introduced to induce near-IR electrochromic properties. One is triphenylamine (TPA) and its derivatives, which are well-known electron-rich compounds and have been widely used as electron-donating and hole-transporting materials in the fields of photovoltaics [26] and electrochromism [27]. Because triphenylamines can easily be oxidized to form TPA cationic radicals with an obvious change of absorption spectrum in the NIR region, it has been reported that TPA can be used to improve the electrochromic performance in the NIR regions [28]. The other one is *p*-diphenylenediamine-containing molecules, which are also excellent anodic electrochromic systems for NIR applications because of its particular low energy intramolecular charge transfer under the oxidized states. Moreover, the *p*-diphenylenediamine cation radical has been reported as a symmetrical delocalized class III structure with a strong electronic coupling, leading to an intervalence charge transfer absorption band in the NIR region [29–31].

In this work, we designed and synthesized a new electrochromic material by substitution of N-position of DTP unit with Ph-TPA group. The novel TPA-containing DTP derives monomer, 4'-(2,5-di(thiophen-2-yl)-1H-pyrrol-1-yl)-N,N-diphenylbiphenyl-4-amine (**DTP-Ph-TPA**; see Scheme 1), was synthesized by Knorr–Paal reaction and SUZUKI coupling reaction, and the corresponding polymer was obtained by electrochemical polymerization. The polymer **PDTP-Ph-TPA** is expected to have excellent electrochromic properties in the visible and NIR region because the DTP section has the variable hues while the TPA section can enhance the NIR electrochromic performance due to its electron sufficiency and hole-transporting properties. Moreover, the two nitrogen atoms in the DTP and TPA groups are connected by diphenylene moiety thus forming a *p*-diphenylenediamine unit, which could further strengthen the absorption spectral in NIR region. Here we demonstrate that the polymer **PDTP-Ph-TPA** exhibits reversible multicolor in the visible region (yellow, light green, magenta and blue) when the applied potential circulates from 0.0 V to 1.4 V. Furthermore, it also shows excellent electrochromic properties in the NIR region with high contrast ratio ( $\Delta T = 70.5\%$  in 1550 nm,  $\Delta T = 67.9\%$

in 1310 nm) and a very short response time (about 1.4 s for 1550 nm, 0.9 s for 1310 nm). Such features are very intriguing in electrochromic materials for wide applications like data storage, optical attenuators, and thermal control (heat gain or loss) in buildings and spacecrafts [32,33].

## 2. Experiments

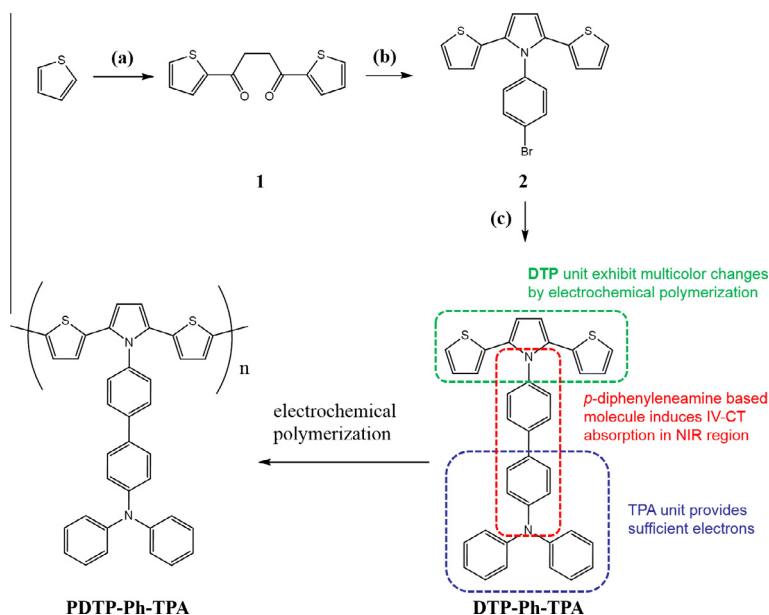
### 2.1. Materials and instrumentation

All reagents and solvents were purchased from commercial sources and used as received without further purification. The solvent used for the electrochemical measurements were purchased from Sigma Aldrich with the purity of HPLC, which include dichloromethane (DCM) and acetonitrile (ACN). The ITO substrates as the working electrode were purchased from Kaivo with the resistance ( $\Omega$ ) below 10  $\Omega$ /sq. Mass spectra were acquired on a time of flight mass spectrometer.  $^1\text{H}$  NMR and  $^{13}\text{C}$  NMR spectra were recorded using a Bruker spectrometer at 500 MHz using TMS as an internal standard. Elemental analyses of the compounds were performed on a Perkin-Elmer 240 analyzer. UV–Vis–NIR spectra were measured on a UV-3600 spectrophotometer. The absorption to the monomer was recorded in DCM with the concentration of  $10^{-5}$  M, and the optical band gap ( $E_g$ ) of the monomer and polymer was calculated from their low-energy absorption edge ( $\lambda_{\text{onset}}$ ) ( $E_g = 1241/\lambda_{\text{onset}}$ ). The cyclic voltammetry (CV) measurement was performed by CHI-660D electrochemical workstation. The measurements were carried out under an argon atmosphere, and the electrochemical three-electrode cell includes a Pt disk ( $d = 0.2$  cm) or ITO (Kaivo,  $<10$   $\Omega$ /sq, 9 mm  $\times$  50 mm) as the working electrode, Pt wire as counter electrode and the Ag wire as the quasi-reference electrode which was calibrated vs  $\text{Fc}/\text{Fc}^+$  to be 0.62 V in DCM solution. 0.1 M  $\text{Bu}_4\text{NClO}_4$  dissolved in DCM was used as electrolyte solution. HOMO and LUMO energy levels of the polymer were calculated according to the Ferrocene/Ferrocenium standard redox couple  $E(\text{Fc}/\text{Fc}^+) = 0.62$  V (vs Ag wire) in DCM by using the formula  $E_{\text{HOMO}} = -e(E^{\text{OX1}} - E_{\text{Fc}}) + (-0.62 \text{ eV})$  [23], and  $\text{LUMO} = \text{HOMO} - E_g$ .

To perform the spectroelectrochemical measurements and electrochromic switching studies, the polymer films were deposited on the ITO by electrochemical polymerization. The measurements were carried out by a spectroelectrochemical cell which consists of a quartz cell with an Ag wire, a Pt wire, and an ITO as the transparent working electrode. 0.1 M  $\text{Bu}_4\text{NClO}_4$  dissolved in DCM was used as electrolyte solution during all the measurement.

### 2.2. Synthetic procedure

The synthesis of the monomer **DTP-Ph-TPA** and corresponding polymer **P-DTP-Ph-TPA** is outlined in Scheme 1. The monomer **DTP-Ph-TPA** was prepared from Paal–Knorr reaction [34,35] and subsequent Suzuki coupling reaction. Succinyl chloride, 4-bromoaniline,  $\text{Pd}(\text{PPh}_3)_4$ , 4-(diphenylamino) phenylboronic acid was purchased from Alfa-Aesar, and used as received. Polymer **PDTP-Ph-TPA** was prepared by electrochemical polymerization.



**Scheme 1.** Synthetic route to the monomer **DTP-Ph-TPA** and polymer **PDTP-Ph-TPA** and the characters of the compound **DTP-Ph-TPA**: (a)  $(\text{CH}_2\text{COCl})_2$ ,  $\text{AlCl}_3$ , DCM, rt, 6 h; (b) 4-bromoaniline, *p*-toluenesulfonic acid monohydrate, toluene,  $\text{Na}_2\text{SO}_4$ , reflux, 36 h; and (c) 4-(diphenylamino)phenylboronic acid,  $\text{Pd}(\text{PPh}_3)_4$ , toluene, reflux, 24 h.

### 2.2.1. Synthesis of 1,4-bis(2'-thienyl)-1,4-butanedione (**1**)

To a suspension of  $\text{AlCl}_3$  (32 g, 0.24 mol) in 90 mL of DCM, a solution of 11 mL (0.1 mol) succinyl chloride and 19.2 mL (0.24 mol) of thiophene in 30 mL DCM was added dropwise at room temperature. The suspension was stirred for 6 h and poured into a mixture of 10 mL of hydrochloric acid and 400 g of ice. The color of the suspension turned from red to dark green after further stirring for 30 min. The organic phase was collected and the aqueous phase was extracted with DCM. The organic phases was combined and washed with water and saturated aqueous  $\text{NaHCO}_3$ , dried over  $\text{NaSO}_4$ , concentrated in vacuo, and purified by column chromatography (eluent:DCM:hexane = 1:1) to afford 14.5 g (58%) of **1** as pale blue crystals.  $^1\text{H}$  NMR (500 MHz,  $\text{CDCl}_3$ ,  $\delta$ , ppm): 7.82 (dd, 2H), 7.65 (dd, 2H), 7.15 (dd, 2H), 3.40 (s, 4H) (Fig. S1). MS (EI) ( $m/z$ ):  $[\text{M}]^+$  calcd for  $\text{C}_{12}\text{H}_{10}\text{O}_2\text{S}_2$ , 250.0; found, 250.1.

### 2.2.2. Synthesis of 1-(4-bromo-phenyl)-2,5-di-thiophene-2-yl-1H-pyrrole (**2**)

A three-neck round-bottomed flask equipped with a Dean-Stark trap, an argon inlet and a reflux condenser, was charged with 1.5 g (6 mmol) compound **1**, 3.01 g (18 mmol) of 4-bromoaniline, 1.25 g (6.6 mmol) of *p*-toluenesulfonic acid monohydrate, 2.5 g  $\text{Na}_2\text{SO}_4$ , and 50 mL toluene. The reaction mixture was stirred and refluxed for 36 h under argon. After cooling to room temperature, toluene was removed by evaporation under reduced pressure. The residue was dissolved in DCM and washed with water and saturated brine. The organic phase was then collected and evaporated under reduced pressure, followed by flash column chromatography ( $\text{SiO}_2$  column, elution with ethyl acetate:hexane = 1:5). The desired product was obtained as pale yellow solid (1.8 g, 78%).  $^1\text{H}$  NMR (500 MHz,  $\text{CDCl}_3$ ,

$\delta$ , ppm): 7.54 (dd, 2H), 7.17 (d, 2H), 7.10 (dd, 2H), 6.85 (dd, 2H), 6.56 (dd, 2H), 6.54 (s, 2H) (Fig. S2). MS (EI) ( $m/z$ ):  $[\text{M}]^+$  calcd for  $\text{C}_{18}\text{H}_{12}\text{NS}_2\text{Br}$ , 385.0; found, 385.1.

### 2.2.3. Synthesis of **DTP-Ph-TPA**

Compound **2** (0.386 g, 1 mmol), 4-(diphenylamino)phenylboronic acid (0.347 g, 1.2 mmol) and  $\text{Pd}(\text{PPh}_3)_4$  (40 mg) were added to a mixture of 2 M  $\text{K}_2\text{CO}_3$  (15 mL) and toluene (20 mL) under argon. The reaction mixture was heated to reflux for 10 h under stirring. After cooled to room temperature and extracted with DCM ( $3 \times 50$  mL), the combined organic phase was washed with water (50 mL) and saturated brine (50 mL). The organic phase was separated and dried over  $\text{Na}_2\text{SO}_4$ . The solvent was removed under reduced pressure and the residue was purified by column chromatography with DCM:hexane = 1:4 as eluent. The final product was obtained as pale yellow crystals (0.41 g, 74%).  $^1\text{H}$  NMR (500 MHz,  $\text{CDCl}_3$ ,  $\delta$ , ppm): 7.65 (d, 2H), 7.56 (d, 2H), 7.33 (d, 2H), 7.28 (dd, 4H), 7.14 (d, 2H), 7.12 (d, 2H), 7.10 (d, 2H), 7.05 (dd, 4H), 6.81 (dd, 2H), 6.60 (d, 2H), 6.53 (s, 2H) (Fig. S3);  $^{13}\text{C}$  NMR (500 MHz,  $\text{CDCl}_3$ ,  $\delta$ , ppm): 135.00, 133.45, 130.28, 129.37, 127.77, 127.03, 126.97, 124.55, 124.29, 124.00, 123.85, 123.18, 109.88 (Fig. S4); MS (EI) ( $m/z$ ):  $[\text{M}]^+$  calcd for  $\text{C}_{36}\text{H}_{26}\text{N}_2\text{S}_2$ , 550.1; found, 550.0. Anal. calcd for  $\text{C}_{36}\text{H}_{26}\text{N}_2\text{S}_2$ : C, 78.51; H, 4.76; N, 5.09; S, 11.64. Found: C, 78.15; H, 4.98; N, 4.96; S, 11.76.

### 2.2.4. Synthesis of polymer **PDTP-Ph-TPA**

The polymerization of the monomer was performed in an electrochemical cell with the presence of 20 mg **DTP-Ph-TPA** and 0.1 M  $\text{Bu}_4\text{NClO}_4$  in 10 ml DCM. The electrochemical cell was equipped with Pt disk ( $d = 0.2$  cm) or ITO glass (whole area was 9 mm  $\times$  50 mm and the active

area was 9 mm × 30 mm) as the working electrode, Pt wire as counter electrode and the Ag wire as the pseudo-reference electrode (calibrated vs Fc/Fc<sup>+</sup>). Before the polymerization, argon was passing through the electrochemical cell for 30 min. Cyclic voltammetry was run between 0.0 V and 1.4 V (vs Fc/Fc<sup>+</sup>) for 30 cycles at room temperature under argon atmosphere. As the polymerization proceeded, the solution became colorful and the uniform film **PDTP-Ph-TPA** whose color was reversible changing with the change of potential was deposited on the working electrode. After the polymerization, the polymer film deposited on the Pt disk or ITO glass was washed with DCM for three times to remove unreacted monomer and residue electrode and then stored in argon.

### 2.3. X-ray structure determination

Yellow needle crystals of complex **DTP-Ph-TPA** were grown in acetonitrile/dichloromethane (*v/v* = 1:1) solution at room temperature. Single-crystal X-ray diffraction measurements were carried out on a Bruker SMART APEX CCD based on a diffractometer operating at room temperature. Intensities were collected with graphite monochromatized Mo K $\alpha$  radiation ( $\lambda$  = 0.71073 Å) operating at 50 kV and 30 mA, in  $\omega/2\theta$  scan mode. The data reduction was made with the Bruker SAINT package [36]. Absorption corrections were performed using the SADABS program [37]. The structures were solved by direct methods and refined on  $F^2$  by full-matrix least-squares using SHELXL-97 with anisotropic displacement parameters for all non-hydrogen atoms in all two structures. Hydrogen atoms bonded to the carbon atoms were placed in calculated positions and refined as riding mode, with C–H = 0.93 Å (methane) or 0.96 Å (methyl) and  $U_{\text{iso}}(\text{H}) = 1.2 U_{\text{eq}}(\text{C}_{\text{methane}})$  or  $U_{\text{iso}}(\text{H}) = 1.5 U_{\text{eq}}(\text{C}_{\text{methyl}})$ . The water hydrogen atoms were located in the difference Fourier maps and refined with an O–H distance restraint [0.85(1) Å] and  $U_{\text{iso}}(\text{H}) = 1.5 U_{\text{eq}}(\text{O})$ . All computations were carried out using the SHELXTL-97 program package [38]. CCDC 1022982 contain the supplementary crystallographic data for this paper. These data can be obtained free of charge from The Cambridge Crystallographic Data Centre via [www.ccdc.cam.ac.uk/data\\_request/cif](http://www.ccdc.cam.ac.uk/data_request/cif).

### 2.4. Fabrication of the electrochromic devices

The structure of the electrochromic device is similar to the literature as reported previously [39–42]. First, a piece of ITO glass (50 mm × 15 mm) was etched with zinc powder and 2 M HCl to get the desired pattern. The etched ITO glass was then washed carefully with DI-water, isopropanol and acetone (Scheme 2a). Oxygen plasma was subsequently used to treat the ITO glass for 10 min. The uniform film **PDTP-Ph-TPA** was deposited electrochemically on the ITO substrate with a DCM solution containing 2 mg/mL **DTP-Ph-TPA** and 0.1 M Bu<sub>4</sub>NClO<sub>4</sub> in an electrochemical cell. Pt wire was used as counter electrode and the Ag wire as the pseudo-reference electrode. The cyclic voltammetry experiment was taken at the potential between 0.0 V and 1.4 V (vs Fc/Fc<sup>+</sup>) for several cycles at room temperature under argon atmosphere (Scheme 2b).

After washed with DCM and dried by argon, the gel electrolyte based on PC/PMMA/LiClO<sub>4</sub>/ACN in a 20:7:3:70 weight ratio was coated on the electrochromic layer (Scheme 2c). The electrochromic and gel electrolyte layers were then surrounded by the Surlyn film (Scheme 2d) and capped with another ITO-coated glass. The two pieces of glass were stuck to each other with Surlyn film by heat sealing, thus forming the typical sandwich structured electrochromic device (Scheme 2e). The cross-section of the electrochromic device was show in Scheme 2f.

## 3. Results and discussions

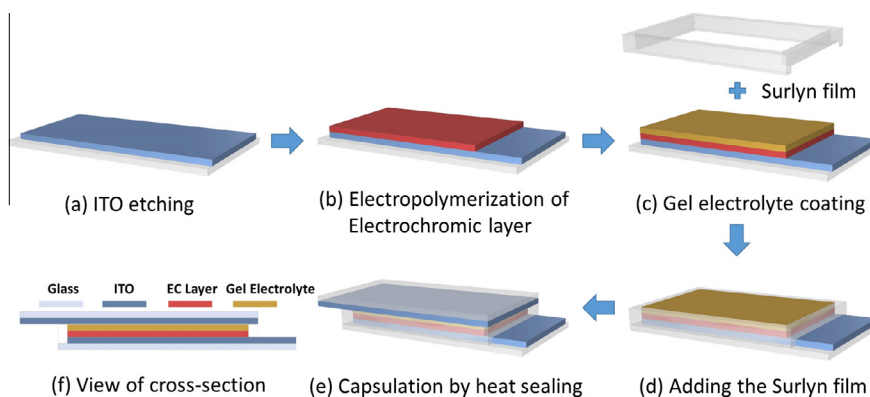
### 3.1. Synthesis and characterization

The new electroactive monomers **DTP-Ph-TPA** which contains TPA as hole transport segment was successfully synthesized by SUZUKI cross coupling reaction of the bromo-compound **2** and 4-(diphenylamino) phenylboronic acid in the presence of Pd(PPh<sub>3</sub>)<sub>4</sub> as catalyst (Scheme 1). The reaction was carried in 2 M K<sub>2</sub>CO<sub>3</sub> and toluene under inertia condition. Compound **2** was synthesized according to the reference via Paal–Knorr reaction of compound **1** with 4-Bromoaniline with the presence of *p*-toluenesulfonic acid as catalyst and dehydrant [34]. In order to accelerate the reaction speed, anhydrous sodium sulfate was added to the reaction mixture. Moreover, a small amount of anhydrous cupric sulfate was added in the Dean-Stark apparatus to track the process of the reaction. Compound **1** was synthesized according to the reference as mentioned above.

The chemical structures of the compound **1**, **2** and **DTP-Ph-TPA** were elucidated by <sup>1</sup>H NMR and EI-MS. The crystal structure of **DTP-Ph-TPA** was determined by single-crystal X-ray diffraction measurements. **DTP-Ph-TPA** crystallizes in orthorhombic crystal system with space group of *Pbnc*. The molecular structure and crystal packing diagram of **DTP-Ph-TPA** are shown in Fig. 1. The crystallographic data was summarized in Table S1, and the bond distances and bond angles were summarized in Table S2. The thienyl moieties are disorder due to their rotation along the C2–C3 single bond (Fig. 1a). There is no  $\pi$ – $\pi$  stacking interaction between the neighboring molecules due to the large steric hindrance of the nonplanar triphenylamine groups.

### 3.2. Electrochemical properties of the **DTP-Ph-TPA**

The electrochemical properties of the monomer **DTP-Ph-TPA** was investigated by CV (Fig. 2a) and differential pulse voltammetry (DPV) (Fig. S5). The CV data was listed in Table 1. During the anodic scan, the monomer **DTP-Ph-TPA** exhibits two oxidation peaks at  $E^{\text{ox}1} = 0.98$  V and  $E^{\text{ox}2} = 1.27$  V vs Ag wire. The first oxidation peak at 0.98 V was attributed to the radical cation (TPA<sup>•+</sup>) formation which was consistent with the reported TPA derivatives [43]. If the anodic potential window was limited to 1.1 V, only one couple of stable quasi-reversible redox peak appeared. The intensity of the peak showed no increase under repetitive cycling. Furthermore, no film was formed



**Scheme 2.** Process for preparing the single layer solid-state electrochromic devices.

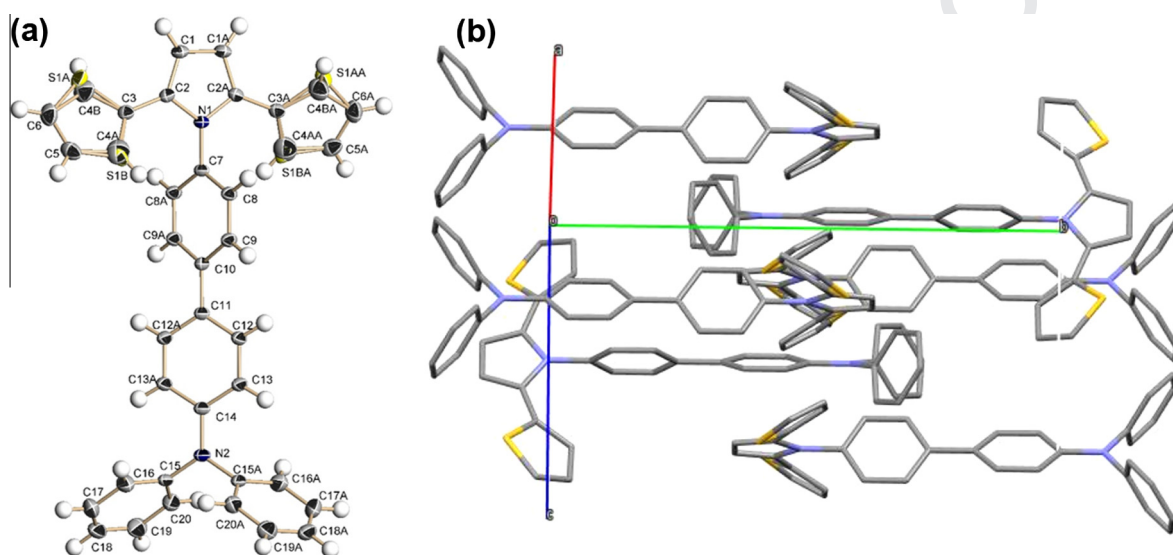


**Fig. 1.** The molecular structure (a) and crystal packing diagram (b) of **DTP-Ph-TPA**.

on the electrode surface via either repetitive cycling or constant potential electrolysis. All these observation are proofs that this couple of peaks belongs to the redox of the TPA unit. When the anodic potential increased to 1.4 V, a new couple of quasi-reversible redox peaks appeared at 1.27 V which can be ascribed to the radical cation formation of DTP unit [22,23]. The negative shift of the potential as compared to other N-substituted DTP derivatives is due to the electron-donating character of the TPA unit [17]. Under repetitive cycling, the intensity of the peaks increased rapidly and there was a colorful film deposited on the electrode surface (Fig. 3a). The energy levels of the HOMO and LUMO of the investigated monomer and polymers can be estimated from the oxidation onset  $E_{\text{onset}}$  according to the following equation

$$\text{HOMO} = E_{\text{onset}} - E_{\text{onset}}(\text{Fc}/\text{Fc}^+) + \text{HOMO}(\text{Fc}/\text{Fc}^+)$$

where the  $E_{\text{onset}}(\text{Fc}/\text{Fc}^+)$  refers to the Ferrocene/Ferrocenium standard redox couple and has a value of 0.62 V (vs Ag wire) in DCM, the standard HOMO energy level of

$\text{Fc}/\text{Fc}^+$  is 4.80 eV. The results are listed in Table 1. The HOMO energy level of the **DTP-Ph-TPA** was 5.01 eV.

To evaluate the adhesive ability of the polymer **PDTP-Ph-TPA** film deposited on the electrode, the peak currents intensities were recorded as a function of scan rates by cyclic voltammetry between 0.0 V and 1.5 V (Fig. 2b). Evidently, the peak currents intensities of the polymer were increased steadily by promoting the scan rates. A linear dependence of the peak currents of anodic and cathodic as a function of scan rates was obtained, and the least square fit were  $R = 0.9942$ ,  $R = 0.9915$ , respectively (Fig. 2c), indicating that the polymer **PDTP-Ph-TPA** film can firmly adhere to the electrode.

### 3.3. Electrochemical polymerization of the **DTP-Ph-TPA**

The electrochemical polymerization of the homopolymer was performed via cyclic voltammetry technique between 0.0 V and 1.4 V,  $-0.2$  V and 1.5 V (vs Ag wire). The polymerization process was carried out in a reaction

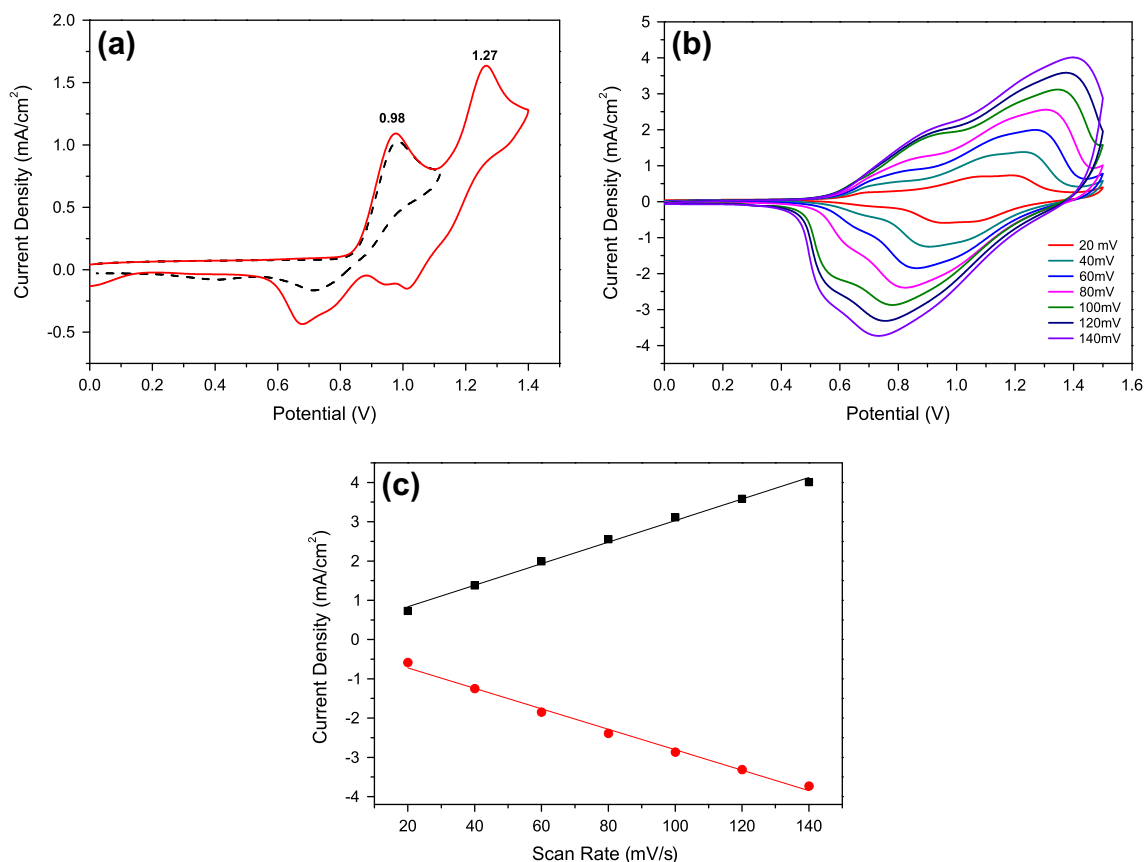


**Fig. 2.** (a) Cyclic voltammograms of **DTP-Ph-TPA** in 0.1 M TBAP/DCM on a platinum electrode vs Ag wire at a scan rate of 100 mV/s (the applied potential of dash line was between 0.0 V and 1.1 V, solid line was between 0.0 V and 1.4 V); (b) scan rate dependence of **PDTP-Ph-TPA** film on a platinum electrode in 0.1 M TBAP/DCM at different scan rates vs Ag wire: 20 mV, 40 mV, 60 mV, 80 mV, 100 mV, 120 mV, 140 mV; and (c) relationship of anodic ( $I_a$ , the black one) and cathodic ( $I_c$ , the red one) peaks as a function of scan rate for **PDTP-Ph-TPA** film in 0.1 M TBAP/DCM. (For interpretation of the references to color in this figure legend, the reader is referred to the web version of this article.)

**Table 1**

Electrochemical properties of monomer and polymer.

Compound	Absorption spectra			Cyclic voltammetry (vs Ag wire)				
	$\lambda_{\max}$ (nm)	$\lambda_{\text{edge}}$ (nm)	$E_g^{\text{opt}}$ (eV) <sup>a</sup>	Oxidation potential (V) <sup>b</sup>			Energy levels (eV)	
				$E_{\text{onset}}$	$E^{\text{ox1}}$	$E^{\text{ox2}}$	HOMO <sup>c</sup>	LUMO <sup>d</sup>
<b>DTP-Ph-TPA</b>	341	410	3.03	0.83	0.98	1.27	5.01	1.98
<b>PDTP-Ph-TPA</b>	360, 440	572	2.17	0.65	0.92	1.33	4.83	2.66

<sup>a</sup> The data were calculated by the equation:  $E_g = 1241/\lambda_{\text{edge}}$  of monomer and polymer films.

<sup>b</sup> Oxidation potentials from cyclic voltammograms vs Ag wire in DCM.

<sup>c</sup> The HOMO energy levels were calculated from cyclic voltammetry and referenced to ferrocene (4.80 eV).

<sup>d</sup> LUMO = HOMO –  $E_g$ .

412 medium containing  $2.0 \times 10^{-3}$  M **DTP-Ph-TPA** and 0.1 M  
 413 TBAP in DCM via repetitive cycling at a scan rate  
 414 100 mV/s (Fig. 3). At the beginning, there were two  
 415 oxidation peaks at 0.98 V and 1.27 V in the first process  
 416 of oxidation which is in agreement with the CV measure-  
 417 ment. When the scan was reversed, two reduction peaks  
 418 with half wave potentials ( $E_{p1/2}$ ) of 0.84 V and 1.16 V,  
 419 respectively, were observed. After the second cycle, there  
 420 was a new oxidation peak at 0.82 V which can be  
 421 attributed to the oxidation of the polymer deposited on

422 the electrode. The intensities of the redox peaks become  
 423 higher and higher under repetitive cycling, indicating that  
 424 an electroactive polymer formed on the electrode surface.

425 In order to investigate the film quality of the polymer,  
 426 the SEM micrographs of polymer films were obtained and  
 427 shown in Fig. 4. The polymer films were synthesized by  
 428 electrochemical polymerization on the ITO substrates and  
 429 peeled off carefully for the SEM measurement. Fig. 4a  
 430 shows that the polymer film exhibits a uniform and  
 431 smooth surface with small pit on it. Fig. 4b was the

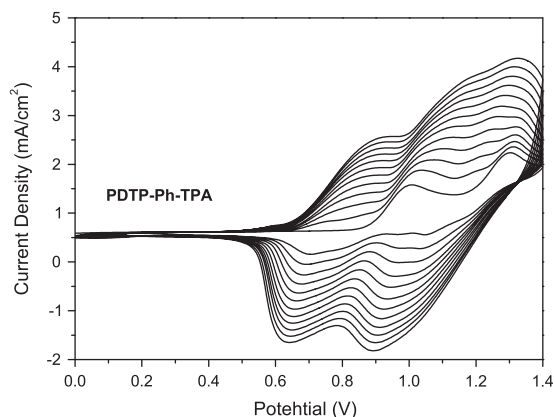


Fig. 3. Electrochemical polymerization of  $2.0 \times 10^{-3}$  M **DTP-Ph-TPA** in 0.1 M TBAP/DCM via repetitive cycling at a scan rate 100 mV/s.

enlargement of the cross section of the film which shows the stratified structure of the polymer with the thickness about 1.0  $\mu\text{m}$ .

### 3.4. Spectroelectrochemical properties

Spectroelectrochemical measurements were conducted by UV–Vis–NIR spectrophotometer upon incrementally changing the applied potential (from 0.0 V to 1.4 V) of the polymer films. In order to remove the doping ion and the residual charge, the polymer films on the ITO were reduced to their neutral state before the measurements of spectroelectrochemical properties. From these measurements, both the optical behavior and electronic structure of the polymer films on the transparent electrode ITO upon *p*-doping can be explained [22].

Fig. 5a and b illustrates the UV–Vis–NIR absorption profiles correlated with applied potentials and the three-dimensional wavelength-potential-absorbance correlation of **PDTP-Ph-TPA** polymer film, respectively. At neutral state, **PDTP-Ph-TPA** polymer is yellow in the visible region and transparent in the NIR regions, with two strong absorption maxima at around 360 nm and 440 nm which

showed a hypsochromic shift compared with the polymer PDTP-Ph [17]. The absorptions were corresponded to the  $\pi$ - $\pi^*$  and  $n$ - $\pi^*$  transitions of the PDTP backbones and the TPA subunits [17]. The band gap  $E_g$  of **PDTP-Ph-TPA** was calculated to be 2.17 eV from the onset of the  $\pi$ - $\pi^*$  transition at 572 nm, which was lower than the precedent PDTP analogs [4]. Upon oxidation of the **PDTP-Ph-TPA** film, the absorption of the  $\pi$ - $\pi^*$  transition at 360 nm gradually decreased while two new absorption at 494 nm and 810 nm as well as a new broad band from 1000 nm to 1650 nm grew up. When the potential was increased to 0.9 V, the absorption at 440 nm decreased to the lowest and the color of the film became green. This potential was associated with the onset of first anodic process in the CV measurements, indicating that the electrons were gradually transporting into the polymer [44]. Upon increasing the potentials to 1.1 V, which corresponds to the first anodic process of **PDTP-Ph-TPA**, the absorption at 494 nm and the broad band at the NIR region became the highest, while the color of the film changed into pink. It is known that the formation of **PDTP-Ph-TPA**<sup>+</sup> radical cation arises from the oxidation of the TPA unit of the polymer [45]. The positive charge of the **PDTP-Ph-TPA**<sup>+</sup> radical cation can transport between the different amino centers of the TPA and DTP through *p*-diphenylenediamine group (Scheme 1), which leads to an intervalence charge transfer of the polymer and exhibits strongest absorption band in the NIR region when the potential increased to 1.1 V [14,31]. Finally, when the potential reached the highest applied potential of 1.4 V, the absorption at 360 nm became the lowest and the new absorption at 810 nm increased to the top, and the color of the film stayed at blue. Meanwhile, the absorption at the NIR region was decreasing, which was consistent with the second anodic process and indicates the further oxidation and formation of **PDTP-Ph-TPA**<sup>2+</sup> dication [45–47]. The absorption band of the **PDTP-Ph-TPA** was reversible when the applied potential was circulated. Fig. 5c illustrates the dynamic spectral changes of **PDTP-Ph-TPA** in % transmittance at 1550, 1310, 810, 494, 440, and 360 nm by changing the applied potentials, which show the maximum optical changes of the electrochromic polymer **PDTP-Ph-TPA** at

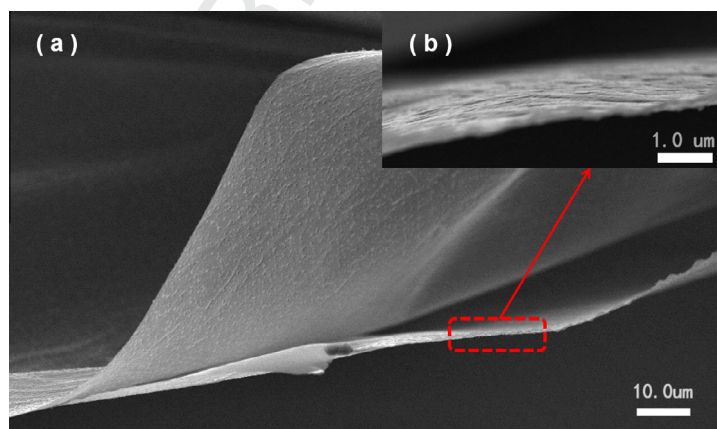
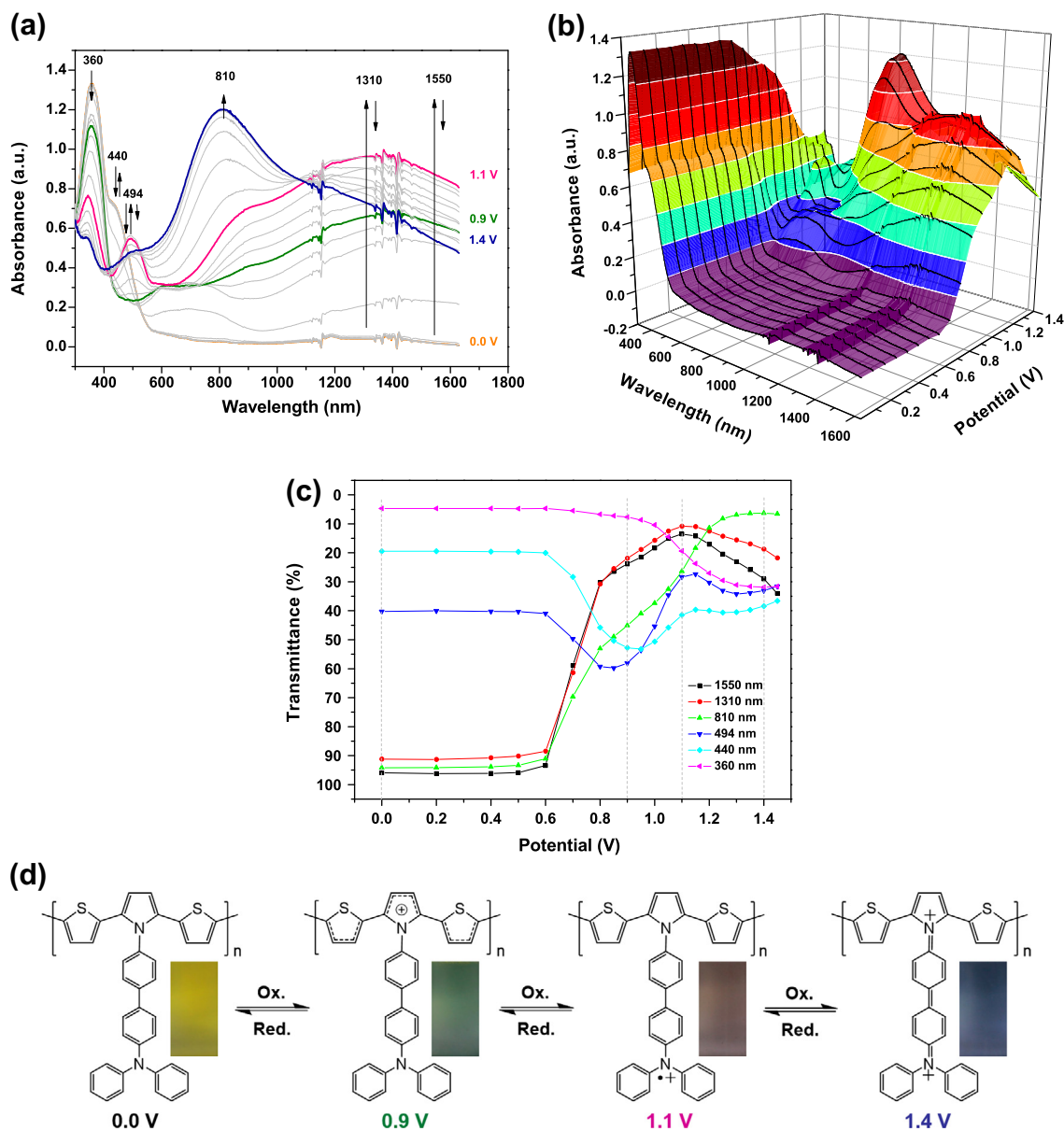


Fig. 4. The SEM micrographs of **PDTP-Ph-TPA** polymer films.



**Fig. 5.** (a) Spectroelectrochemical properties of homo-polymer **PDTP-Ph-TPA** thin film on the ITO in 0.1 M TBAP/DCM at various applied potentials (from 0.0 to 1.4); (b) 3-D spectroelectrochemical behavior from 0.0 to 1.4 V (vs Ag wire) of **PDTP-Ph-TPA** thin film on the ITO in 0.1 M TBAP/DCM; (c) optical change in T% as a function of applied potential for six absorption bands at 1550, 1310, 810, 494, 440 and 360 nm; and (d) the illustration of the chemical structure with color changes of **PDTP-Ph-TPA** as a function of applied potentials. (For interpretation of the references to color in this figure legend, the reader is referred to the web version of this article.)

495 the appropriate step potentials. Fig. 5d illustrates the  
496 chemical structure with color changes (from yellow to  
497 light green to magenta and blue) of **PDTP-Ph-TPA** as a  
498 function of applied potentials.

### 499 3.5. Electrochromic switching

500 For electrochromic switching studies, **PDTP-Ph-TPA**  
501 was deposited on ITO glass by electrochemical polymeriza-  
502 tion as described above. Chronoamperometric and absor-  
503 bance measurements were performed. The absorbance of

504 the polymer films at the given wavelength was monitored  
505 as a function of time with UV-Vis-NIR spectroscopy when  
506 the film was switched between different potential. Switch-  
507 ing data of **PDTP-Ph-TPA** at 1550 nm and 1310 nm were  
508 shown in Fig. 6a and b. The switching time of the polymer  
509 was calculated at 90% of the ultimate contrast because it  
510 is difficult to perceive any further color change with naked  
511 eye beyond this limit. As showed in Fig. 5, the applied  
512 potential of **PDTP-Ph-TPA** was switched between 0.0 and  
513 1.1 V. When the detective wavelength was 1550 nm  
514 (Fig. 6a), **PDTP-Ph-TPA** revealed switching time of 2.8 s

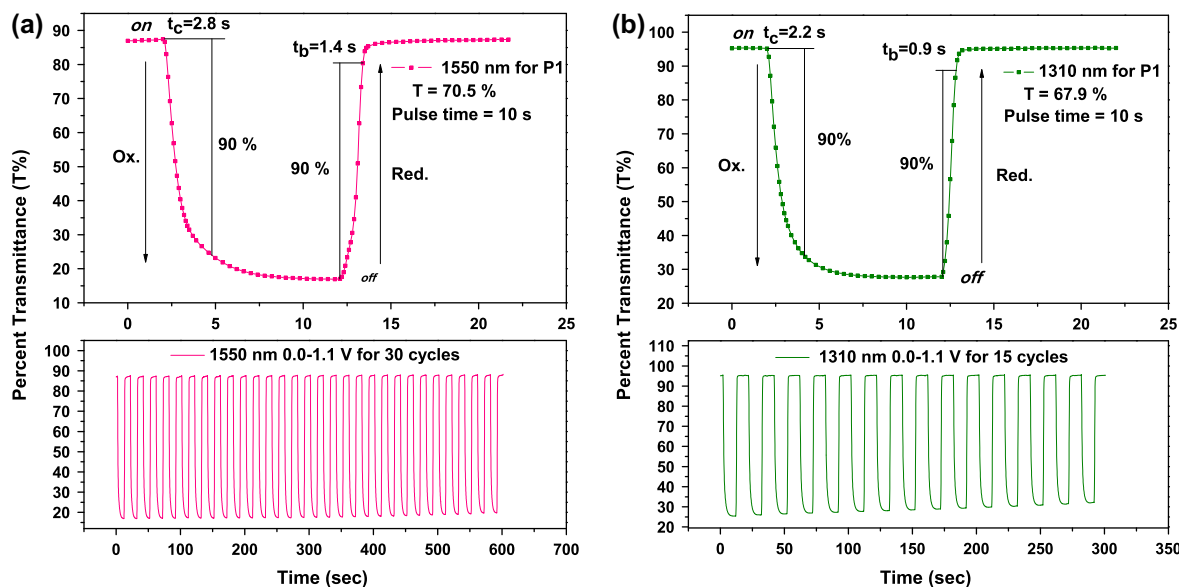


**Fig. 6.** Potential step absorptiometry of the polymer film **PDTP-Ph-TPA** on the ITO (coated area:  $2 \text{ cm}^2$ ) in 0.1 M TBAP/DCM.  $\lambda_{\text{max}} = 1550 \text{ nm}$  (a) and  $1310 \text{ nm}$  (b) with the applied potential stepped between 0.0 V and 1.1 V at a cycle time of 20 s ( $t_c$  = coloring time,  $t_b$  = bleaching time).

**Table 2**

Summary of kinetic studies of **PDTP-Ph-TPA**.

	$\lambda$ (nm)	Optical contrast			$t_c$ (s)	$t_b$ (s)	$\Delta\text{OD}$	$Q_d$ (C/cm $^2$ )	CE (cm $^2$ /C)
		$T_b$	$T_c$	$\Delta T\%$					
<b>PDTP-Ph-TPA</b>	1550	87.44	16.93	70.51	2.8	1.4	0.6196	0.004966	125.72
	1310	95.29	25.47	69.82	2.2	0.9	0.5730	0.003083	185.86
	810	61.83	8.65	53.18	3.0	1.1	0.8542	0.008307	102.83

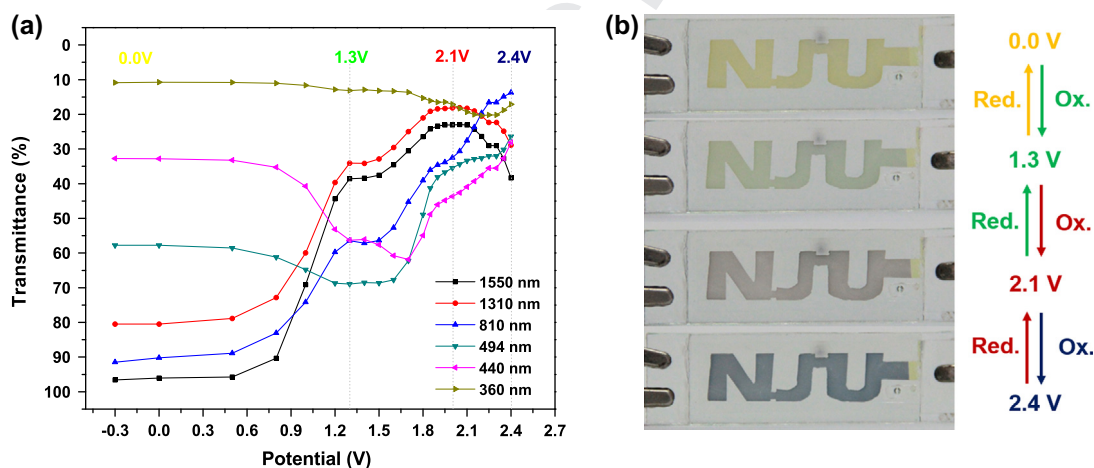


**Fig. 7.** (a) Optical change in %T as a function of applied potential for six absorption bands at 1550, 1310, 810, 494, 440 and 360 nm; and (b) the photo shows the color change of electrochromic devices at different applied potentials.

515 for coloring process ( $t_c$ ) and 1.4 s for bleaching ( $t_b$ ) at the  
 516 transmittance of 70.5%. When the detective wavelength  
 517 was 1310 nm (Fig. 6b), **PDTP-Ph-TPA** requires 2.2 s for  
 518 coloration and 0.9 s for bleaching at the transmittance of  
 519 67.9%. The polymer showed a faster bleaching process in

comparison with the coloring process, which was because  
 520 the polymer has a faster kinetics of dopant ion diffusion in  
 521 the reduction process than for the reverse process [25,48].  
 522 Moreover, **PDTP-Ph-TPA** shows reversible optical changes  
 523 upon switching between its neutral and oxidation states.  
 524

The switching time and transmittance for other wavelengths of the polymer film **PDTP-Ph-TPA** were listed in Table 2, and the details were showed in supplementary data (Fig. S6).

The coloration efficiency (CE) is one of the important parameters for the electrochromic materials. The CE of the polymer films is equal to the ratio of optical density change ( $\Delta OD$ ) to the amount of injected/ejected charge ( $Q_d$ ), and it can be calculated by utilizing the following equations [49]

$$CE(\lambda) = \Delta OD(\lambda)/Q_d \text{ and } \Delta OD(\lambda) = \log[T_c(\lambda)/T_b(\lambda)]$$

where  $T_c$  and  $T_b$  are the percent transmittance of coloring and bleaching state, respectively. The CE of the polymers **PDTP-Ph-TPA** at various wavelengths was listed in Table 2.

### 3.6. Performance of electrochromic devices

In order to investigate the dynamic performance of the polymer, a single layer window-type electrochromic device was prepared from **PDTP-Ph-TPA**. The fabricated devices were successfully switched from their neutral to oxidized states at 0.0–2.4 V. The dynamic spectral changes of the fabricated devices in transmittance percentage at 1550, 1310, 810, 494, 440, and 360 nm by changing the applied potentials are showed in Fig. 7a, which shows the maximum optical changes of the electrochromic devices at the appropriate step potentials. Fig. 7b shows the different color changes at different applied potential, which is consistent with the hue changes of polymer **PDTP-Ph-TPA** film which was deposited on the ITO.

## 4. Conclusion

In summary, we designed and synthesized a new electrochromic material by substitution of N-position of DTP unit with TPA group. The three sections in the **DTP-Ph-TPA** molecule have different function: the DTP section has the variable hues, the TPA section enhances the NIR electrochromic performance due to its electron sufficiency and hole-transporting properties, while the *p*-diphenylenediamine section further strengthens the absorption spectral in NIR. The resulting homopolymer **PDTP-Ph-TPA** not only exhibit reversible multicolor in the visible region (yellow, light green, magenta, cyan and blue), but also shows excellent electrochromic properties in the NIR region which perform a high contrast ratio ( $\Delta T = 70.5\%$  in 1550 nm,  $\Delta T = 67.9\%$  in 1310 nm) and a very short response time (about 1.4 s for 1550 nm, 0.9 s for 1310 nm). Such materials would be an outstanding material for electrochromic and have wide applications like data storage, active optical filters, and thermal control (heat gain or loss) in buildings and spacecrafts.

## Acknowledgments

This work was supported by the National Natural Science Foundation of China (91022031, 21021062), Major State Basic Research Development Program (Grant Nos. 2013CB922100, 2011CB933303, and 2011CB808704), and

Doctoral Fund of Ministry of Education of China (20120091130002).

## Appendix A. Supplementary material

Supplementary data associated with this article can be found, in the online version, at <http://dx.doi.org/10.1016/j.orgel.2014.10.033>.

## References

- 1) A.A. Argun, P.-H. Aubert, B.C. Thompson, I. Schwendeman, C.L. Gaupp, J. Hwang, N.J. Pinto, D.B. Tanner, A.G. MacDiarmid, J.R. Reynolds, Multicolored electrochromism in polymers: structures and devices, *Chem. Mater.* 16 (2004) 4401–4412.
- 2) P.M. Monk, R.J. Mortimer, D.R. Rosseinsky, *Electrochromism and Electrochromic Devices*, Cambridge University Press Cambridge, UK, 2007.
- 3) P.M. Beaujuge, S. Ellinger, J.R. Reynolds, The donor–acceptor approach allows a black-to-transmissive switching polymeric electrochrome, *Nat. Mater.* 7 (2008) 795–799.
- 4) P.M. Beaujuge, J.R. Reynolds, Color control in  $\pi$ -conjugated organic polymers for use in electrochromic devices, *Chem. Rev.* 110 (2010) 268–320.
- 5) R.J. Mortimer, *Electrochromic materials*, *Annu. Rev. Mater. Res.* 41 (2011) 241–268.
- 6) Y.-W. Zhong, C.-J. Yao, H.-J. Nie, Electropolymerized films of vinyl-substituted polypyridine complexes: synthesis, characterization, and applications, *Coord. Chem. Rev.* 257 (2013) 1357–1372.
- 7) L. Beverina, G.A. Pagani, M. Sassi, Multichromophoric electrochromic polymers: colour tuning of conjugated polymers through the side chain functionalization approach, *Chem. Commun.* 50 (2014) 5413–5430.
- 8) X. You, *Molecular-Based Materials-Opto-electronic Functional Compounds*, second ed., Science Press, Beijing, 2014.
- 9) A.L. Dyer, C.R.G. Grenier, J.R. Reynolds, A poly(3,4-alkylenedioxythiophene) electrochromic variable optical attenuator with near-infrared reflectivity tuned independently of the visible region, *Adv. Funct. Mater.* 17 (2007) 1480–1486.
- 10) J. Zheng, W.Q. Qiao, X.H. Wan, J.P. Gao, Z.Y. Wang, Near-infrared electrochromic and chiroptical switching materials: design, synthesis, and characterization of chiral organogels containing stacked naphthalene diimide chromophores, *Chem. Mater.* 20 (2008) 6163–6168.
- 11) H.-J. Yen, G.-S. Liou, Solution-processable novel near-infrared electrochromic aromatic polyamides based on electroactive tetraphenyl-*p*-phenylenediamine moieties, *Chem. Mater.* 21 (2009) 4062–4070.
- 12) H.-J. Yen, H.-Y. Lin, G.-S. Liou, Novel Starburst triarylamine-containing electroactive aramids with highly stable electrochromism in near-infrared and visible light regions, *Chem. Mater.* 23 (2011) 1874–1882.
- 13) L.-T. Huang, H.-J. Yen, J.-H. Wu, G.-S. Liou, Preparation and characterization of near-infrared and multi-colored electrochromic aramids based on aniline-derivatives, *Org. Electron.* 13 (2012) 840–849.
- 14) Y.W. Chuang, H.J. Yen, J.H. Wu, G.S. Liou, Colorless triphenylamine-based aliphatic thermoset epoxy for multicolored and near-infrared electrochromic applications, *ACS Appl. Mater. Interfaces* 6 (2014) 3594–3599.
- 15) B.B. Cui, C.J. Yao, J.N. Yao, Y.W. Zhong, Electropolymerized films as a molecular platform for volatile memory devices with two near-infrared outputs and long retention time, *Chem. Sci.* 5 (2014) 932–941.
- 16) Y. Liu, D. Chao, H. Yao, New triphenylamine-based poly(amine-imide)s with carbazole-substituents for electrochromic applications, *Org. Electron.* 15 (2014) 1422–1431.
- 17) S. Tarkuc, E. Sahmetlioglu, C. Tanyeli, I.M. Akhmedov, L. Toppare, A soluble conducting polymer: 1-phenyl-2,5-di(2-thienyl)-1H-pyrrole and its electrochromic application, *Electrochim. Acta* 51 (2006) 5412–5419.
- 18) E. Yildiz, P. Camurlu, C. Tanyeli, I. Akhmedov, L. Toppare, A soluble conducting polymer of 4-(2,5-di(thiophen-2-yl)-1H-pyrrol-1-yl)benzenamine and its multichromic copolymer with EDOT, *J. Electroanal. Chem.* 612 (2008) 247–256.

- [19] G. Wang, X. Fu, J. Huang, C.L. Wu, L. Wu, J. Deng, Q. Du, X. Zou, Syntheses and electrochromic and fluorescence properties of three double dithienylpyrroles derivatives, *Electrochim. Acta* 56 (2011) 6352–6360.
- [20] M.P. Algi, Z. Öztas, S. Tirkes, A. Cihaner, F. Algi, A new electrochromic copolymer based on dithienylpyrrole and EDOT, *Org. Electron.* 14 (2013) 1094–1102.
- [21] S. Tirkes, J. Mersini, Z. Öztas, M.P. Algi, F. Algi, A. Cihaner, A new processable and fluorescent polydithienylpyrrole electrochrome with pyrene appendages, *Electrochim. Acta* 90 (2013) 295–301.
- [22] S. Koyuncu, O. Usluer, M. Can, S. Demic, S. Icli, N. Serdar, Sariciftci, Electrochromic and electroluminescent devices based on a novel branched multi-electrochromic materials: enhancing the electrochromic performance via longer side alkyl chain, *J. Mater. Chem.* 21 (2011) 2684.
- [23] F. Baycan Koyuncu, E. Sefer, S. Koyuncu, E. Ozdemir, The new branched multi-electrochromic materials: enhancing the electrochromic performance via longer side alkyl chain, *Macromolecules* 44 (2011) 8407–8414.
- [24] P. Camurlu, Z. Bicil, C. Gültekin, N. Karagoren, Novel ferrocene derivatized poly(2,5-dithienylpyrrole)s: optoelectronic properties, electrochemical copolymerization, *Electrochim. Acta* 63 (2012) 245–250.
- [25] G. Wang, X. Fu, J. Huang, L. Wu, J. Deng, Synthesis, electrochemical and fluorescence properties of three new dithienylpyrroles bearing aromatic amine units, *J. Electroanal. Chem.* 661 (2011) 351–358.
- [26] S. Ryu, J.H. Noh, N.J. Jeon, Y. Chan Kim, W.S. Yang, J. Seo, S.I. Seok, Voltage output of efficient perovskite solar cells with high open-circuit voltage and fill factor, *Energy Environ. Sci.* 7 (2014) 2614.
- [27] S.O. Hacıoglu, S. Toksabay, M. Sendur, L. Toppare, Synthesis and electrochromic properties of triphenylamine containing copolymers: effect of  $\pi$ -bridge on electrochemical properties, *J. Polym. Sci., Part A: Polym. Chem.* 52 (2014) 537–544.
- [28] J. Natera, L. Otero, L. Sereno, F. Fungo, N.-S. Wang, Y.-M. Tsai, T.-Y. Hwu, K.-T. Wong, A novel electrochromic polymer synthesized through electropolymerization of a new donor–acceptor bipolar system, *Macromolecules* 40 (2007) 4456–4463.
- [29] M.B. Robin, P. Day, *Adv. Inorg. Chem. Radiochem.* 10 (1967) 247–422.
- [30] C. Lambert, G. Noll, The class II/III transition in triarylamine redox systems, *J. Am. Chem. Soc.* 121 (1999) 8434–8442.
- [31] S.-H. Hsiao, H.-M. Wang, S.-H. Liao, Redox-stable and visible/near-infrared electrochromic aramids with main-chain triphenylamine and pendent 3,6-di-tert-butylcarbazole units, *Polym. Chem.* 5 (2014) 2473.
- [32] C.-G. Granqvist, Electrochromic materials: out of a niche, *Nat. Mater.* 5 (2006) 89–90.
- [33] F.C. Krebs, Electrochromic displays: the new black, *Nat. Mater.* 7 (2008) 766–767.
- [34] K.-S. Kim, M.-S. Kang, H. Ma, A.K.Y. Jen, Highly efficient photocurrent generation from a self-assembled monolayer film of a novel c60-tethered 2,5-dithienylpyrrole triad, *Chem. Mater.* 16 (2004) 5058–5062.
- [35] J. Nakazaki, I. Chung, M.M. Matsushita, T. Sugawara, R. Watanabe, A. Izuoka, Y. Kawada, Design and preparation of pyrrole-based spin-polarized donors electronic supplementary information (ESI) available: cyclic voltammograms for N-PN,  $\beta$ -PN, N-TPN, PhNN and TPP. *J. Mater. Chem.*, 13 (2003) 1011–1022 <<http://www.rsc.org/suppdata/jm/b2/b211986b>>.
- [36] SAINT-Plus, version 6.02, Bruker Analytical X-ray System, Madison, WI, 1999.
- [37] S.G.M. Sheldrick, An Empirical Absorption Correction Program, Bruker Analytical X-ray Systems, Madison, WI, 1996.
- [38] B.A. Shelxtl, W. Madison, CrossRef CAS PubMed; GM Sheldrick, SHELX-97, *Acta Crystallogr. Sect. A: Fundam. Crystallogr.* 64 (2008) 112–122.
- [39] M.A. Invernale, Y. Ding, D.M.D. Mamangun, M.S. Yavuz, G.A. Sotzing, Preparation of conjugated polymers inside assembled solid-state devices, *Adv. Mater.* 22 (2010) 1379–1382.
- [40] D. Navarathne, W.G. Skene, Towards electrochromic devices having visible color switching using electronic push–push and push–pull cinnamaldehyde derivatives, *ACS Appl. Mater. Interfaces* 5 (2013) 12646–12653.
- [41] L. Sicard, D. Navarathne, T. Skalski, W. Skene, On-substrate preparation of an electroactive conjugated polyazomethine from solution-processable monomers and its application in electrochromic devices, *Adv. Funct. Mater.* 23 (2013) 3549–3559.
- [42] H.-M. Wang, S.-H. Hsiao, Ambipolar, multi-electrochromic polypyromellitimides and polynaphthalimides containing di(tert-butyl)-substituted bis(triarylamine) units, *J. Mater. Chem. C* 2 (2014) 1553.
- [43] W.-H. Chen, K.-L. Wang, W.-Y. Hung, J.-C. Jiang, D.-J. Liaw, K.-R. Lee, J.-Y. Lai, C.-L. Chen, Novel triarylamine-based alternating conjugated polymer with high hole mobility: synthesis, electro-optical, and electronic properties, *J. Polym. Sci., Part A: Polym. Chem.* 48 (2010) 4654–4667.
- [44] D.J. Irvin, C.J. DuBois Jr., J.R. Reynolds, Dual p- and n-type doping in an acid sensitive alternating bi(ethylenedioxythiophene) and pyridine polymer, *Chem. Commun.* (1999) 2121–2122.
- [45] S.-H. Hsiao, G.-S. Liou, Y.-C. Kung, H.-J. Yen, High contrast ratio and rapid switching electrochromic polymeric films based on 4-(dimethylamino)triphenylamine-functionalized aromatic polyamides, *Macromolecules* 41 (2008) 2800–2808.
- [46] G.S. Liou, C.W. Chang, Highly stable anodic electrochromic aromatic polyamides containing N,N,N',N'-tetraphenyl-p-phenylenediamine moieties: synthesis, electrochemical, and electrochromic properties, *Macromolecules* 41 (2008) 1667–1674.
- [47] S.-H. Hsiao, H.-M. Wang, P.-C. Chang, Y.-R. Kung, T.-M. Lee, Synthesis and electrochromic properties of aromatic polyetherimides based on a triphenylamine-dietheramine monomer, *J. Polym. Sci., Part A: Polym. Chem.* 51 (2013) 2925–2938.
- [48] C. Pozo-Gonzalo, M. Salsamendi, J.A. Pomposo, H.J. Grande, E.Y. Schmidt, Y.Y. Rusakov, B.A. Trofimov, Influence of the introduction of short alkyl chains in poly(2-(2-thienyl)-1H-pyrrole) on its electrochromic behavior, *Macromolecules* 41 (2008) 6886–6894.
- [49] B.D. Reeves, C.R.G. Grenier, A.A. Argun, A. Cirpan, T.D. McCarley, J.R. Reynolds, Spray coatable electrochromic dioxathiophene polymers with high coloration efficiencies, *Macromolecules* 37 (2004) 7559–7569.

704  
705  
706  
707  
708  
709  
710  
711  
712  
713  
714  
715  
716  
717  
718  
719  
720  
721  
722  
723  
724  
725  
726  
727  
728  
729  
730  
731  
732  
733  
734  
735  
736  
737  
738  
739  
740  
741  
742  
743  
744  
745  
746  
747  
748  
749  
750  
751  
752  
753  
754  
755  
756  
757  
758